Molecular Basis of Cell and Developmental Biology:

Endophilin B1/Bif-1 Stimulates BAX Activation Independently from Its Capacity to Produce Large Scale Membrane Morphological Rearrangements

Aitor Etxebarria, Oihana Terrones, Hirohito Yamaguchi, Ane Landajuela, Olatz Landeta, Bruno Antonsson, Hong-Gang Wang and Gorka Basañez

J. Biol. Chem. 2009, 284:4200-4212.
doi: 10.1074/jbc.M808050200 originally published online December 11, 2008

THE JOURNAL OF BIOLOGICAL CHEMISTRY VOL. 284, NO. 7, pp. 4200–4212, February 13, 2009

Endophilin B1/Bif-1 Stimulates BAX Activation Independently from Its Capacity to Produce Large Scale Membrane Morphological Rearrangements*[S]

Received for publication, October 21, 2008, and in revised form, December 5, 2008 Published, JBC Papers in Press, December 11, 2008, DOI 10.1074/jbc.M808050200

Aitor Etxebarria[‡1], Oihana Terrones[‡1], Hirohito Yamaguchi[§], Ane Landajuela[‡], Olatz Landeta[‡], Bruno Antonsson[¶], Hong-Gang Wang[‖], and Gorka Basañez[‡2]

From the [‡]Unidad de Biofísica, Centro Mixto Consejo Superior de Investigaciones Cientificas, Universidad del Pais Vasco/Euskal Herriko Unibertsitatea, P. O. Box 644, 48080 Bilbao, Spain, the [§]University of Texas M. D. Anderson Cancer Center, Houston, Texas 77030, [¶]Merck Serono International S. A., 9 chemin des Mines, 1202 Geneva, Switzerland, and the [‖]Department of Pharmacology, Penn State College of Medicine, Hershey, Pennsylvania 17033

Endophilin B1/BAX-interacting factor 1 (Bif-1) is a protein that cooperates with dynamin-like protein 1 (DLP1/Drp1) to maintain normal mitochondrial outer membrane (MOM) dynamics in healthy cells and also contributes to BAX-driven MOM permeabilization (MOMP), the irreversible commitment point to cell death for the majority of apoptotic stimuli. However, despite its importance, exactly how Bif-1 fulfils its proapoptotic role is unknown. Here, we demonstrate that the stimulatory effect of Bif-1 on BAX-driven MOMP and on BAX conformational activation observed in intact cells during apoptosis can be recapitulated in a simplified system consisting of purified proteins and MOM-like liposomes. In this reconstituted model system the N-BAR domain of Bif-1 reproduced the stimulatory effect of Bif-1 on functional BAX activation. This process was dependent on physical interaction between Bif-1 N-BAR and BAX as well as on the presence of the mitochondrion-specific lipid cardiolipin. Despite that Bif-1 N-BAR produced large scale morphological rearrangements in MOM-like liposomes, this phenomenon could be separated from functional BAX activation. Furthermore, DLP1 also caused global morphological changes in MOM-like liposomes, but DLP1 did not stimulate BAX-permeabilizing function in the absence or presence of Bif-1. Taken together, our findings not only provide direct evidence for a functional interplay between Bif-1, BAX, and cardiolipin during MOMP but also add significantly to the growing body of evidence indicating that components of the mitochondrial morphogenesis machinery possess proapoptotic functions that are independent from their recognized roles in normal mitochondrial dynamics.

MOMP[3] is a key event in the intrinsic pathway of mammalian apoptosis, resulting in the release of several apoptogenic proteins from the mitochondrial intermembrane space into the cytosol (1). Released intraorganellar components, including cytochrome *c*, Smac/DIABLO, and AIF, then act as mediators for activating executioner caspase proteases or for other downstream events in the intracellular apoptosis cascade. MOMP is tightly regulated by BCL-2 family members, whose core components are proapoptotic BAX-type proteins that directly effect MOMP and antiapoptotic BCL-2-type proteins which inhibit MOMP (2, 3). In a currently popular model, a third subgroup of BCL-2 family proteins, the BH3-only proteins, trigger a set of conformational changes in BAX and/or its close homologue BAK that activates their permeabilizing function, thereby causing MOMP.

Multiple proteins implicated in mitochondrial morphogenesis during normal growth conditions can cross-talk with BCL-2 family members to affect the mitochondrial pathway of apoptosis (4). For example, the large dynamin-like GTPase DLP1/Drp1 and hFis1, two essential components of the mitochondrial fission machinery, have been shown to modulate pro-apoptotic BAX function and mitochondrial cytochrome *c* release by acting at the level of the MOM (5–7). However, although excessive mitochondrial fragmentation is characteristic in mammalian apoptosis, controversy persists as to whether this phenomenon is merely coincident with or causatively linked to MOMP induction (4–8). In addition, a considerable body of evidence has amassed indicating that DLP1/Drp1 and hFis1 are multifunctional proteins that do not use the same mechanisms to reshape mitochondria in healthy conditions and to promote release of mitochondrial intermembrane space proteins during apoptosis (7–10).

* This work was supported by Ministerio de Ciencia e Innovación Grants BFU2008-01637 (to G. B.) and CA82197-09 (to H.-G. W.). The costs of publication of this article were defrayed in part by the payment of page charges. This article must therefore be hereby marked "*advertisement*" in accordance with 18 U.S.C. Section 1734 solely to indicate this fact.

[S] The on-line version of this article (available at http://www.jbc.org) contains supplemental Figs. 1–4 and Table 1.

[1] Recipients of predoctoral fellowships from the Basque Government.

[2] To whom correspondence should be addressed: Unidad de Biofísica (CSIC-UPV/EHU), Barrio Sarriena s/n, Leioa 48940, Spain. Tel.: 34-94-6013355; Fax: 34-94-6013360; E-mail: gbzbaasg@lg.ehu.es.

[3] The abbreviations used are: MOMP, mitochondrial outer membrane (MOM) permeabilization; LUV, large unilamellar vesicles; OG, β-octylglucoside; D70, fluorescein isothiocyanate-labeled dextrans of 70 kDa; PC, phosphatidylcholine; PE, phosphatidylethanolamine; PI, phosphatidylinositol; CL, heart cardiolipin; mirCL, miristoyl CL; MCL, monolysocardiolipin; DCL, dilysocardiolipin; CD, circular dichroism; DLS, dynamic light scattering; FRET, fluorescence resonance energy transfer; Bif-1, BAX-interacting factor 1; NBD, 12-(*N*-methyl-*N*-(7-nitrobenz-2-oxa-1,3-diazol-4-yl); GTPγS, guanosine 5′-3-*O*-(thio)triphosphate; CHAPS, 3-[(3-cholamidopropyl)dimethylammonio]-1-propanesulfonic acid; BBM, BAX binding motif.

Endophilin B1/BAX-interacting factor 1 (Bif-1) is another protein linking mitochondrial morphological changes and BCL-2-regulated programmed cell death (4). On the one hand, Bif-1 is known to participate downstream of DLP1/Drp1, modulating normal MOM morphological dynamics in healthy cells (11). On the other hand, in response to specific apoptotic signals, a significant portion of Bif-1 binds BAX at the MOM in close temporal correlation with BAX conformational change and cytochrome *c* release (12). In addition, increasing the levels of Bif-1 has been shown to accelerate BAX conformational change, caspase activation, and apoptotic cell death, whereas loss of Bif-1 delays all these processes (12, 13). Together, these previous findings point to an important contributing role of Bif-1 in BAX-driven MOMP during apoptosis, but the underlying molecular mechanism remains unknown.

As other members of the endophilin family, Bif-1 contains an N-BAR (Bin-amphiphysin-Rvs) domain that has been shown to confer ability to these proteins for transforming flat lipid bilayers into high curvature buds, tubules, and vesicles *in vitro* (14–17). Crystallographic studies of the N-BAR domain of endophilin A1, a close homologue of Bif-1, revealed a crescent-shape homodimer with a positively charged concave surface which is believed to act like a molecular scaffold that impresses its own curvature on binding to negatively charged membranes (16, 18). Another distinguishing feature of endophilin N-BAR domains is the presence of two distinct amphipathic segments referred to as "Helix 0" (H0) and "Helix 1 insert" (H1I) that penetrate only partway into the external leaflet and are thought to create a wedge effect that also increases membrane curvature. This dual curvature-generating mechanism has been linked to the shared capacity of endophilins to operate in membrane tubulovesicular dynamics during normal cell growth together with dynamin/dynamin-like proteins (16–18). However, exactly how the molecular-scale perturbation of membrane curvature induced by N-BAR domains translates into large scale membrane remodeling processes (*e.g.* tubulation and vesiculation) is not well understood (19–25). In addition, it is unclear whether the ability of Bif-1 to produce global changes in membrane morphology is functionally connected to its apoptotic mode of action.

The complexity of the network of intermolecular interactions that controls the BCL-2-regulated MOMP pathway constitutes a major hurdle for gaining a molecular-level understanding of Bif-1 pro-death function in intact cells. Another complicating factor is that Bif-1 can interact with binding partners other than BAX at intracellular membranes distinct from the MOM depending on environmental conditions (14, 26–29). In previous studies this and other laboratories have shown that the BCL-2-regulated MOMP pathway can be reconstituted in a simplified system consisting of purified recombinant proteins and chemically defined MOM-like large unilamellar vesicles (LUV) in a manner that faithfully reflects the basic physiological functions of BCL-2 family proteins at the MOM (30–33). Here, we have used this minimal cell-free system to advance our understanding of the pro-death role of Bif-1. We provide strong evidence for a direct implication of Bif-1 in functional BAX activation at the membrane level and novel insights concerning the mechanism through which Bif-1 achieves this effect.

EXPERIMENTAL PROCEDURES

Materials—Egg phosphatidylcholine (PC), egg phosphatidylethanolamine (PE), liver phosphatidylinositol (PI), heart cardiolipin (CL), myristoylated cardiolipin (myrCL), monolysocardiolipin (MCL), dilysocardiolipin (DCL), *N*-(NBD)-phosphatidylethanolamine), and *N*-(lissamine rhodamine B sulfonyl) phosphatidylethanolamine were purchased from Avanti Polar Lipids (Alabaster, AL). KCl, HEPES, EDTA, dodecyl octaethylene glycol monoether ($C_{12}E_8$), Triton X-100, β-octylglucoside (OG), tetanolysin, GTP, GTPγS, and fluorescein isothiocyanate-labeled dextrans of 70 kDa (FD70) were obtained from Sigma. Disuccinimidyl suberate was purchased from Molecular Probes (Eugene, OR).

Recombinant Proteins and Synthetic Peptides—Recombinant full-length human BAX with an amino-terminal His_6 tag (BAX) (31), caspase 8-cleaved murine BID with an amino-terminal His_6 tag (tBID) (31), recombinant human Bcl-X_L lacking the carboxyl-terminal 24 amino acids and with an amino-terminal His_6 tag (BCL-X_L) (31), recombinant rat dynamin-like protein 1 with an amino-terminal His_6 tag (DLP1) (34), and recombinant human Fis1 lacking the carboxyl-terminal 31 amino acids and with an amino-terminal His_6 tag (hFis1) (34) were purified as previously described. OG-BAX was obtained by incubating BAX with 2% OG (w/v) for 1 h at 4 °C. The recombinant human Bif-1 proteins were purified using IMPACT system (New England Biolabs). In brief, the human Bif-1, Bif-1 (1–252), and Bif-1 (253–361) cDNAs were amplified by PCR and subcloned into pTYB1 vector (New England Biolabs) with NdeI and SapI sites. The resulting plasmids, which express Bif-1 and intein-tag fusion proteins, were transformed into BL21 *Escherichia coli*. Recombinant proteins were isolated by a chitin affinity chromatography according to the manufacturer's protocol. The Bif-1 proteins were cleaved off from intein tag by dithiothreitol and dialyzed in 10 mM Hepes (pH 7.4), 100 mM NaCl, and 0.2 mM EDTA. All proteins were purified from soluble fractions of bacterial extracts obtained in the absence of detergents and were >90% pure as evaluated by Coomassie-stained SDS-PAGE (supplemental Fig. 1). High performance liquid chromatography-purified peptides were obtained from Abgent (San Diego, CA). Peptide identity was confirmed by electrospray mass spectroscopy.

Cytochrome c Release Assays—Mitochondria were isolated from livers of male Harlan Sprague-Dawley rats as described previously (31). Isolated mitochondria (500 μg of protein/ml) were incubated with recombinant proteins in 125 mM KCl, 5 mM KH_2PO_4, 2 mM $MgCl_2$, 25 μM EGTA, 5 mM succinate, 5 μM rotenone, and 10 mM HEPES-KOH (pH 7.2) for 20 min at 30 °C under constant stirring using an Eppendorf Thermomixer (V_{final} = 100 μl). Reaction mixtures were centrifuged at 14,000 × *g* for 10 min. Supernatant fractions and pellet fractions were subjected to 4–20% SDS-PAGE followed by Western blotting using anti-cytochrome *c* 7H8.2C-12 antibody (Pharmingen). Mitochondria were kept on ice and used within 3 h of preparation (R&D Systems, Minneapolis, MN).

Liposome Preparation—Unless otherwise indicated, liposomes were prepared with a lipid composition resembling that of MOM contact sites ((40 PC/35 PE/10 PI/15 CL (mol/mol)) (MOM-like liposomes). Lipid mixtures at the indicated ratios were co-dissolved in chloroform/methanol (2:1), and organic solvents were removed by evaporation under an argon stream followed by incubation under vacuum for 2 h. For membrane permeabilization assays, dry lipid films were resuspended in 100 mM KCl, 10 mM Hepes (pH 7.0), 0.1 mM EDTA (KHE buffer) supplemented with 100 mg/ml FD70. For other assays dry lipid films were resuspended in KHE. Multilamellar vesicles were then subjected to 5 freeze/thaw cycles. Except where indicated, these frozen/thawed liposomes were then extruded 10 times through two polycarbonate membranes of 0.2-μm pore size (Nucleopore, San Diego, CA) to obtain LUV. Untrapped FD70 was removed by gel filtration in Sephacryl S-500 HR columns with KHE running as elution buffer.

Fluorimetric Measurements of Vesicular Contents Release—Release of LUV-encapsulated FD70 was monitored in an 8100 Aminco-Bowman luminescence spectrometer (Spectronic Instruments, Rochester, NY) in a thermostatically controlled 1-cm path length cuvette with constant stirring at 37 °C (V_{final} = 750 μl). The FD70 emission was monitored at 525 nm with the excitation wavelength set at 490 nm (slits, 4 nm). A cutoff filter at 515 nm was used between the sample and the emission monochromator to avoid scattering interferences. The extent of marker release was quantified on a percentage basis according to the equation ($F_t - F_0/F_{100} - F_0$) = 100 where F_t is the measured fluorescence of protein-treated LUV at time t, F_0 is the initial fluorescence of the LUV suspension before protein addition, and F_{100} is the fluorescence value after complete disruption of LUV by the addition of $C_{12}E_8$ (final concentration, 0.5 mM). Lipid concentration was 50 μM.

Fluorimetric Measurements of Intervesicular Lipid Mixing—Membrane lipid mixing was monitored using the fluorescence resonance energy transfer (FRET) assay described by Struck *et al.* (35). The assay is based on the dilution of the NBD-PE/*N*-(lissamine rhodamine B sulfonyl)-PE FRET pair. LUV containing 2 mol % of each probe were mixed with unlabeled vesicles at a 1:10 ratio. Dilution of the fluorescent probes due to membrane fusion resulted in an increased NBD-PE fluorescence. The NBD emission was monitored at 530 nm with the excitation wavelength set at 465 nm. A cutoff filter at 515 nm was used between the sample and the emission monochromator to avoid scattering interferences. The fluorescence scale was calibrated such that the zero level corresponded to the initial residual fluorescence of the labeled vesicles and the 100% value corresponded to complete mixing of all the lipids in the system. The latter value was set by the fluorescence intensity upon the addition of 10 mM OG. Proteins were incubated with LUV (50 μM) for 10 min in a thermostatically controlled 1-cm path length cuvette with constant stirring at 37 °C (V_{final} = 750 μl) followed by determination of extents of intervesicular lipid mixing.

Binding of Proteins to MOM-like Liposomes—To assess the liposome binding capacity of an individual protein in a mixture containing multiple proteins, a low speed vesicle sedimentation approach was used followed by detection of the protein of interest by immunoblotting. In brief, proteins were incubated with freeze/thawed vesicles (100 μM) for 30 min at 37 °C under constant stirring using an Eppenford Thermomixer (V_{final} = 100 μl). Next, the mixture was centrifuged for another 30 min at 18,000 × *g* at 4 °C, and equivalent aliquots were taken from the supernatant (corresponding to free protein) and pellet fractions (corresponding to liposome-bound protein). Both fractions were then subjected to reducing SDS-PAGE on 15% Tris-glycine gels followed by protein visualization by immunoblotting using anti BAX N20 polyclonal antibody (Santa Cruz) or anti-Bif-1 monoclonal antibody (Imgenex).

Assays of BAX Oligomerization at MOM-mimetic LUV—For studies of BAX oligomerization, apoptotic proteins were first incubated with MOM-mimetic LUV (100 μM) for 30 min at 37 °C under constant stirring using an Eppendorf Thermomixer (V_{final} = 100 μl). Then, disuccinimidyl suberate cross-linker was added at 0.1 mM concentration followed by incubation of the mixture for 30 min at room temperature and quenching of free cross-linker by addition of 0.1 volume of 2 M Tris-HCl (pH 7.4). Finally, samples were examined for BAX immunoreactivity with anti-BAX N20 antibody.

Immunoprecipitations—Proteins were incubated with LUV (100 μM) in KHE buffer for 30 min at 37 °C under constant stirring using an Eppendorf Thermomixer (V_{final} = 300 μl) followed by the addition of CHAPS (0.5% w/v, final concentration) and immunoprecipitation with agarose-conjugated anti-BAX N20 antibody (Santa Cruz) for 2 h at 4 °C on a rotator. Immunoprecipitates were collected by centrifugation (5 min, 5000 × *g*). The pellets were washed 2 times with KHE supplemented with 2% CHAPS (w/v), then an additional 2 times with KHE. Immunoprecipitates were released from the beads in SDS loading buffer and analyzed for Bif-1 immunoreactivity.

Far-UV Circular Dichroism (CD) Measurements—Far-UV CD spectra were recorded at 37 °C on a Jasco J-810 spectrapolarimeter (Jasco Spectroscopic Co. Ltd., Hachioji City, Japan) equipped with a JASCO PTC-423S temperature control unit using a 1-mm path length cell. Data were collected every 0.2 nm at 50 nm/min from 250 to 200 nm with a bandwidth of 2 nm, and results were averaged from 20 scans. For experiments with liposomes, small unilamellar vesicles were obtained by sonication to diminish the contribution from scattered light. Bif-1^{1-252}, Bif-1^{1-27}, and lipid concentrations were 5 μM, 20 μM, and 2 mM, respectively. All samples were allowed to equilibrate for 10 min before CD analysis. Each spectrum represents the average of three distinct spectral recordings. The contribution of buffer with/or without small unilamellar vesicles to the measured ellipticity was subtracted as blank. Molar ellipticity values (ϕ) were calculated using the expression $\phi = \epsilon/10cnl$, where ϵ is the ellipticity (millidegrees), c is the protein concentration (mol/liter), l is the cuvette path length, and n is the number of amino acid residues in the protein. The amount of secondary structural elements was estimated with the CD-Pro software.

Monolayer Surface Pressure Measurements—Surface pressure measurements were carried out with a MicroTrough-S system from Kibron (Helsinki, Finland) with constant stirring at 37 °C. Lipid monolayers were prepared with a lipid composition resembling that of MOM contact sites (40 PC/35 PE/10 PI/15 CL (mol/mol)) (MOM-like monolayers). The lipid, dissolved in chloroform and methanol (2:1), was gently spread

over the surface of 1-ml KHE buffer and kept at a constant surface area. The desired initial surface pressure was attained by changing the amount of lipid applied to the air-water interface. After 10 min to allow for solvent evaporation, compounds of interest were injected through a hole connected to the subphase, and the change in surface pressure was recorded as a function of time until a stable signal was obtained. Under these conditions maximal surface pressures obtained after injecting compounds in the absence of a lipid monolayer were below initial monolayer pressure values examined.

DLS Measurements—Vesicle size was determined by DLS at a fixed angle of 90° and 37 °C using a Protein Solutions DynaPro instrument equipped with a temperature-controlled microchamber and a 64-channel correlator capable of estimating particle sizes in the range from 5 to 5000 nm. LUV (50 μM) were incubated with or without proteins in KHE buffer for 10 min at 37 °C under constant stirring using an Eppendorf Thermomixer (V_{final} = 70 μl) followed by DLS analysis. Each measurement was done as an average of 20 data points and took approximately between 15 and 20 min. Data were analyzed by the cumulant method using the software provided by the instrument.

RESULTS

Bif-1 Stimulates BAX-permeabilizing Function in MOM-like LUV—We began by examining the capacity of purified full-length recombinant human Bif-1 (termed Bif-1 hereafter) to release mitochondrial cytochrome *c* either by itself or in combination with BAX or with tBID-activated BAX. Incubation of isolated rat liver mitochondria with Bif-1 either alone or in combination with BAX produced minimal release of cytochrome *c*, whereas treatment of organelles with a BAX plus tBID mixture produced near-to-complete release of cytochrome *c* (Fig. 1*A*, *left*). However, the addition of Bif-1 to isolated mitochondria treated with BAX together with a suboptimal dosing of tBID produced an enhancement in the amount of cytochrome *c* release (Fig. 1*A*, *middle*), and this effect could be blocked by antiapoptotic BCL-X_L (Fig. 1*A*, *right*). One possible explanation for these results is that Bif-1 increases the degree of MOMP under suboptimal BAX-activating conditions by directly potentiating the permeabilizing function of BAX. To test this hypothesis, we switched to a quantitative liposome release assay that faithfully reproduces basic aspects of the BAX-driven MOMP pathway in which MOM-like LUV are preloaded with FD70. As observed with isolated mitochondria, the addition of Bif-1 alone or Bif-1 plus BAX to MOM-like LUV caused minimal release of vesicular FD70, whereas the addition of Bif-1 to BAX combined with a suboptimal amount of tBID strongly stimulated vesicular dextran release (Fig. 1*B*). Also as seen with mitochondria, the stimulatory effect of Bif-1 on vesicular dextran release could be inhibited by BCL-X_L (Fig. 1*C*), suggesting that Bif-1 causes vesicular leakage by potentiating the physiologically relevant BAX-permeabilizing function rather than via an alternative mechanism. We recently demonstrated that exposure to heat directly activates BAX-permeabilizing function in MOM-like LUV (31). Bif-1 also stimulated vesicular FD70 release when BAX was exposed to a suboptimal temperature in a BCL-X_L-inhibitable manner, indicating that

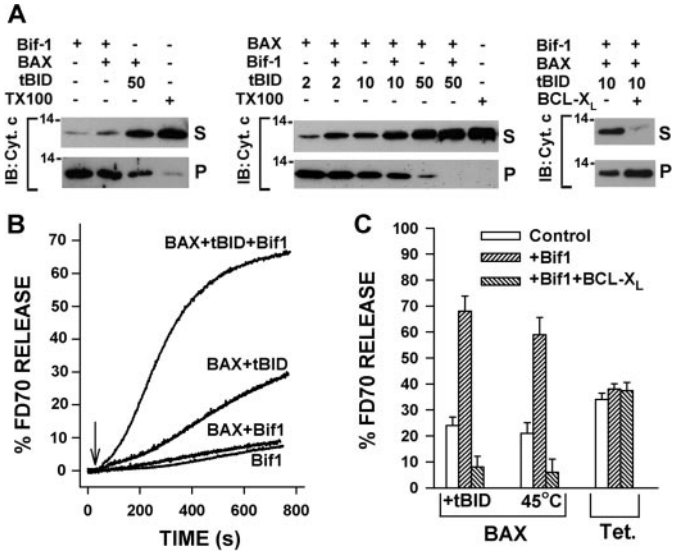

FIGURE 1. **Bif-1 stimulates BAX-permeabilizing function in MOM-like liposomes.** *A*, Bif-1 potentiates mitochondrial cytochrome *c* release induced by tBID-activated BAX. Freshly isolated rat liver mitochondria were treated with indicated recombinant proteins, samples were subjected to centrifugation, and the resulting supernatants (*S*) and pellet (*P*) fractions were analyzed by SDS-PAGE/immunoblotting (*IB*) using anti-cytochrome *c* (*cyt. c*) antibody. BAX, Bif-1, and BCL-X_L concentrations were 50, 200, and 500 nM, respectively. Total cytochrome *c* release was determined by Triton X-100 (*TX100*, 1 mM) solubilization of mitochondria. *B*, Bif-1 potentiates vesicular FD70 release induced by tBID-activated BAX. Representative time courses of FD70 release from MOM-like LUVs elicited by indicated recombinant apoptotic proteins. BAX, tBID, and Bif-1 concentrations were 50, 10, and 200 nM, respectively. The *arrow* denotes time of protein addition to the liposome suspension. *C*, extents of vesicular FD70 release induced by BAX plus tBID, BAX exposed to 45 °C, or tetanolysin (*Tet.*) in the absence (*Control*) or presence of Bif-1 or BCL-X_L. Data were taken 10 min after protein addition. Concentrations of BAX, tBID, Bif-1, BCL-X_L, and tetanolysin were 50, 10, 200, 500, and 5 nM, respectively. Data represent mean values and S.E. of at least two independent experiments.

tBID is not required for Bif-1-mediated enhancement of BAX-permeabilizing function (Fig. 1*C*). Additional supporting evidence for the specificity of Bif-1-mediated stimulation of BAX-permeabilizing function in MOM-like LUV was provided by the finding that Bif-1 had little impact on the vesicular contents release induced by tetanolysin, a cholesterol-dependent channel unrelated to BAX (Fig. 1*C*).

Next, we sought to determine whether Bif-1 interacts with BAX in this reconstituted liposomal system, as expected from results observed during apoptosis in intact cells (12, 13, 36). Immunoprecipitates were prepared using anti-BAX antibodies and subjected to SDS-PAGE/immunoblot assays using anti-Bif-1 antibodies, revealing robust coimmunoprecipitation of Bif-1 with tBID-activated BAX in the presence of MOM-like LUV but not in the absence of lipid vesicles (Fig. 2*A*). Moreover, in correlation with results obtained in dextran release assays, elimination of tBID from the reaction mixture markedly reduced the amount of Bif-1 that could be coimmunoprecipitated with BAX.

The BAX-induced membrane permeabilization process has been proposed to consist of several events, which include (i) recruitment of BAX to the membrane, (ii) oligomerization of BAX at the membrane plane, and (iii) opening/expansion of a BAX-lipid pore (32). Thus, we next examined the effect of Bif-1 at each one of these steps in the BAX-driven membrane permeabilization pathway. To assess the impact of Bif-1 on BAX bind-

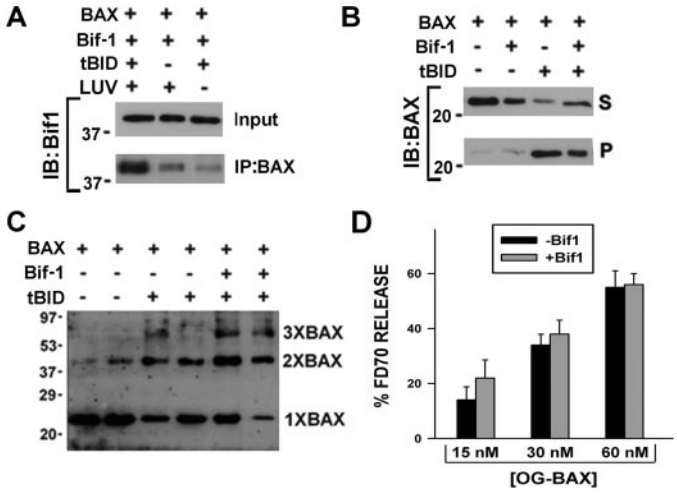

FIGURE 2. **Bif-1 interacts with BAX and stimulates BAX oligomerization in MOM-like liposomes.** *A*, BAX with or without tBID was incubated with Bif-1 and MOM-like liposomes. Samples were subjected to immunoprecipitation (*IP*) with anti-BAX antibody conjugated to agarose beads followed by SDS-PAGE/immunoblot (*IB*) analysis of Bif-1. Concentrations of BAX, tBID, and Bif-1 were 100, 20, and 400 nM, respectively. *B*, immunoblot analysis of BAX recruitment to MOM-like liposomes. Freeze/thawed vesicles were treated with the indicated proteins followed by centrifugation of the mixture and immunodetection of BAX contents in the liposome-containing pellet (*P*) and liposome-free supernatant (*S*) fractions. Protein concentrations were as explained in *panel A*. *C*, effect of Bif-1 on BAX oligomerization. Duplicated samples were prepared in which MOM-like liposomes were incubated with indicated proteins followed by treatment with disuccinimidyl suberate cross-linker and assessment of BAX oligomerization by immunoblotting. Protein concentrations were as explained in *panel A*. *D*, effect of Bif-1 (200 nM) on the vesicular FD70 release induced by increasing amounts of OG-treated BAX. Data represent the mean values and S.E. from two independent measurements.

ing to MOM-like liposomes, the vesicles were incubated with BAX alone or with a mixture of BAX plus a suboptimal dosing of tBID in the presence or absence of Bif-1. Then, liposome-containing and liposome-devoid fractions were separated by centrifugation, and the amounts of liposome-bound BAX (pellet (*P*)) and free BAX (supernatant (*S*)) were analyzed by SDS-PAGE/immunoblotting. As shown in Fig. 2*B*, the amount of BAX recruited to the liposomes appeared unaffected by the presence of Bif-1. Next, we examined whether Bif-1 has any impact on BAX oligomerization. After incubation of apoptotic proteins with MOM-like liposomes, samples were treated with the cross-linker disuccinimidyl suberate and analyzed for BAX by SDS-PAGE/immunoblotting. As shown in Fig. 2*C*, in the absence of other proteins BAX was primarily present in a monomeric form. Incubation of MOM-like LUV with a suboptimal tBID concentration shifted BAX into higher-order cross-linked BAX adducts. Importantly, the addition of Bif-1 to the mixture containing BAX and a suboptimal dosing of tBID increased the amount of BAX in higher-order oligomeric forms, indicating that Bif-1 potentiates BAX oligomerization under these experimental conditions. When BAX was exposed to a suboptimal activation temperature, Bif-1 also increased the amount of higher-order oligomeric BAX species without apparently affecting BAX membrane recruitment, suggesting that Bif-1 does not require tBID to stimulate conformational activation of membrane-associated BAX (supplemental Fig. 2). To further test whether Bif-1 acts by promoting BAX oligomerization, we examined the effect of Bif-1 on the permeabilizing function of OG-treated BAX, a fully active form of BAX that spontaneously adopts an intramembranous oligomeric fold upon interaction with MOM-like LUV. As shown in Fig. 2*D*, unlike the situation found in conditions of suboptimal BAX activation, Bif-1 had little effect on vesicular dextran release when added in combination with OG-treated BAX.

These findings led us to the following two conclusions. First, the stimulatory effect of Bif-1 on BAX-driven MOMP and the Bif-1:BAX interaction observed in intact cells can be recapitulated in a simplified system consisting of purified recombinant proteins and MOM-like liposomes. Second, in this compositionally defined cell-free system, Bif-1 seems to act by promoting BAX acquisition of an active fold within the plane of the membrane rather than by facilitating BAX membrane recruitment or formation/expansion of the BAX-lipid pore.

Bif-1 Stimulates Functional BAX Activation via Its N-BAR Domain through a CL-dependent Mechanism—All endophilins have a similar overall structure consisting of the following domains: first, a relatively conserved N-BAR domain that comprises the amino-terminal two-thirds of the molecule; second, a carboxyl-terminal Src homology 3 (SH3) domain; third, a variable region (*VR*) linking the N-BAR and SH3 domains (Fig. 3*A*). Additionally, yeast two-hybrid studies indicated that the BAX binding motif (BBM) of Bif-1 encompasses a short sequence stretch at the N terminus of the protein including part of the H0 submodule of the N-BAR domain (37). To identify the region of Bif-1 required for stimulation of BAX-permeabilizing function, we generated deletion mutants lacking the variable region plus Src homology 3 (Bif-1^{1-252}) or N-BAR domains (Bif-$1^{253-361}$) and a synthetic peptide representing the first 27 amino acids of Bif-1 encompassing the BBM and the entire H0 submodule of the N-BAR domain (Bif-1^{1-27}). Dose dependence assays showed that Bif-1^{1-252} fully retains the stimulatory effect of Bif-1 on BAX-induced vesicular dextran release, whereas Bif-$1^{253-361}$ and Bif-1^{1-27} were unable to stimulate BAX-permeabilizing function (Fig. 3*B*). Bif-1^{1-252} also reproduced the ability of the full-length protein to stimulate BAX oligomerization in the presence of MOM-like LUV (supplemental Fig. 2).

Interestingly, despite its incapacity to bind BAX in solution as assessed by fluorescence polarization assays (supplemental Table 1), pretreatment of MOM-like LUV with increasing amounts of Bif-1^{1-27} progressively diminished the stimulatory effect of Bif-1^{1-252} on BAX-induced vesicular dextran release (Fig. 3*C*). In contrast, pretreatment of MOM-like LUV with an equivalent endophilin A1 peptide (EndA1^{1-27}), which lacks a BBM, did not affect Bif-1^{1-252}-mediated stimulation of BAX-permeabilizing function. We interpret these results as indicative that Bif-1^{1-27} competes with Bif-1^{1-252} for binding BAX in the presence of MOM-like LUV, thereby inhibiting the stimulatory effect elicited by Bif-1^{1-252} on BAX-induced vesicular dextran release. Consistent with this interpretation, Bif-1^{1-252} could be immunoprecipitated with BAX in the presence of MOM-like LUV, and preincubation of liposomes with Bif-1^{1-27}, but not EndA1^{1-27} peptide, severely diminished this interaction (Fig. 3*D*).

Apart from their ability to engage in interactions with selected protein partners, N-BAR domains are known for their capacity to interact with membrane lipids (38). Therefore, we

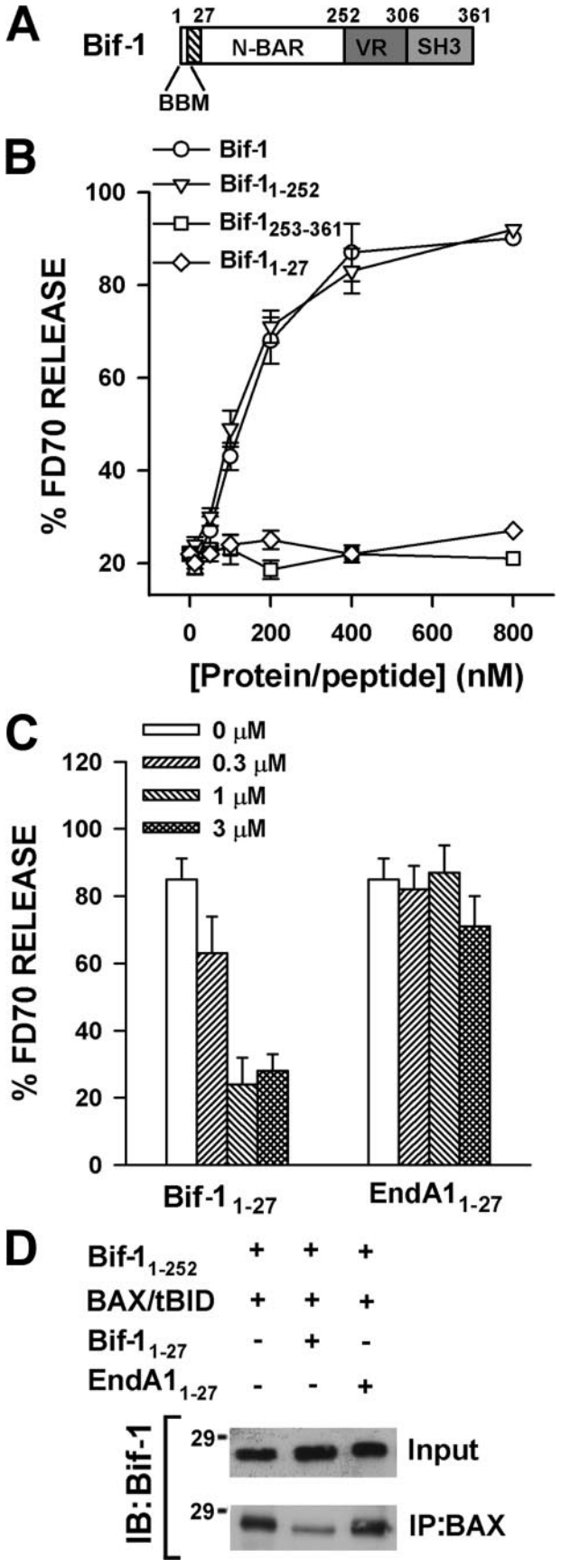

FIGURE 3. **Bif-1 N-BAR domain reproduces the stimulatory effect of Bif-1 on BAX-permeabilizing function.** *A*, schematic representation of the domain structure of Bif-1, indicating the number of amino acid residue positions of the various domains and the H0 submodule (*striped box*). The BBM is indicated *below* the *diagram*. *B*, dose dependence of the effects elicited by Bif-1 and fragments derived thereof on the vesicular FD70 release induced by tBID-activated BAX. BAX and tBID concentrations were 50 and 10 nM, respectively. Data represent the mean values and S.E. of 3–5 independent measurements. *C*, MOM-like LUV were pretreated with indicated amounts of synthetic peptides for 5 min followed by the addition of BAX (50 nM), tBID (10 nM), and Bif-1^{1-252} (200 nM). Extents of vesicular FD70 release were determined after further incubating the mixtures for 10 min. Data represent the mean values and S.E. of duplicated measurements. *D*, MOM-like LUV were incubated with or without indicated peptides (4 μM) for 5 min followed by the addition of BAX (100 nM), tBID (20 nM), and Bif-1^{1-252} (400 nM) and further incubation of the mixtures. Samples were then immunoprecipitated (*IP*) using anti-BAX antibody conjugated to agarose beads and immunoblotted (*IB*) for Bif-1.

next evaluated the influence of individual lipids of the MOM-like mixture in Bif-1-mediated potentiation of BAX-permeabilizing function. Strikingly, removing the mitochondrion-specific lipid CL from MOM-like LUV nearly abolished the stimulatory effect elicited by Bif-1 on BAX-driven vesicular FD70 release, whereas eliminating either PE or PI had little effect on liposome permeability (Fig. 4*A*). The behavior of Bif-1^{1-252} was indistinguishable from that of the full-length protein, indicating that the lipid specificity for potentiation of BAX-permeabilizing function is encoded within the Bif-1 N-BAR domain. Importantly, elimination of CL from MOM-like LUV produced minimal changes in the ability of Bif-1^{1-252} to interact with the lipid vesicles (Fig. 4*B*) or to coimmunoprecipitate with BAX (Fig. 4*C*).

These findings led us to the following conclusions. First, Bif-1 activates BAX-permeabilizing function via its N-BAR domain. Second, Bif-1 interacts with BAX via the most N-terminal part of the N-BAR domain. Third, CL plays a crucial role in the potentiation of BAX-permeabilizing function by Bif-1 N-BAR domain.

The Ability of Bif-1 N-BAR to Produce Large Scale Morphological Rearrangements in MOM-like LUV Can Be Uncoupled from Its Stimulatory Effect on BAX-permeabilizing Function—Because interactions between N-BAR-containing proteins and anionic liposomes can produce global changes in vesicle morphology (14–17), we next examined whether Bif-1 possesses the ability to modify the morphology of MOM-like LUV and whether this property is mechanistically linked to potentiation of BAX-permeabilizing function. Previous studies demonstrated that the endophilin A1 H0 segment undergoes a disorder-to-helix transition upon contacting pure lipid vesicles and that this process is an important contributor of its ability for transforming spherical liposomes into elongated membrane tubes (17). Hence, we performed CD measurements on Bif-1^{1-252} and Bif-1^{1-27} in solution and in the presence of MOM-like liposomes with or without CL. As expected from results obtained with endophilin A1, the addition of MOM-like liposomes increased the helical content of Bif-1 N-BAR and shifted Bif-1^{1-27} from being unstructured to adopting a helical fold (Fig. 5 and Table 1). Importantly, however, the CD spectra and helical contents of Bif-1^{1-252} and Bif-1^{1-27} remained virtually unaltered upon removal of CL from the MOM-like lipid mixture.

Another property of endophilin A1 thought to contribute to large scale rearrangements in membrane morphology is the

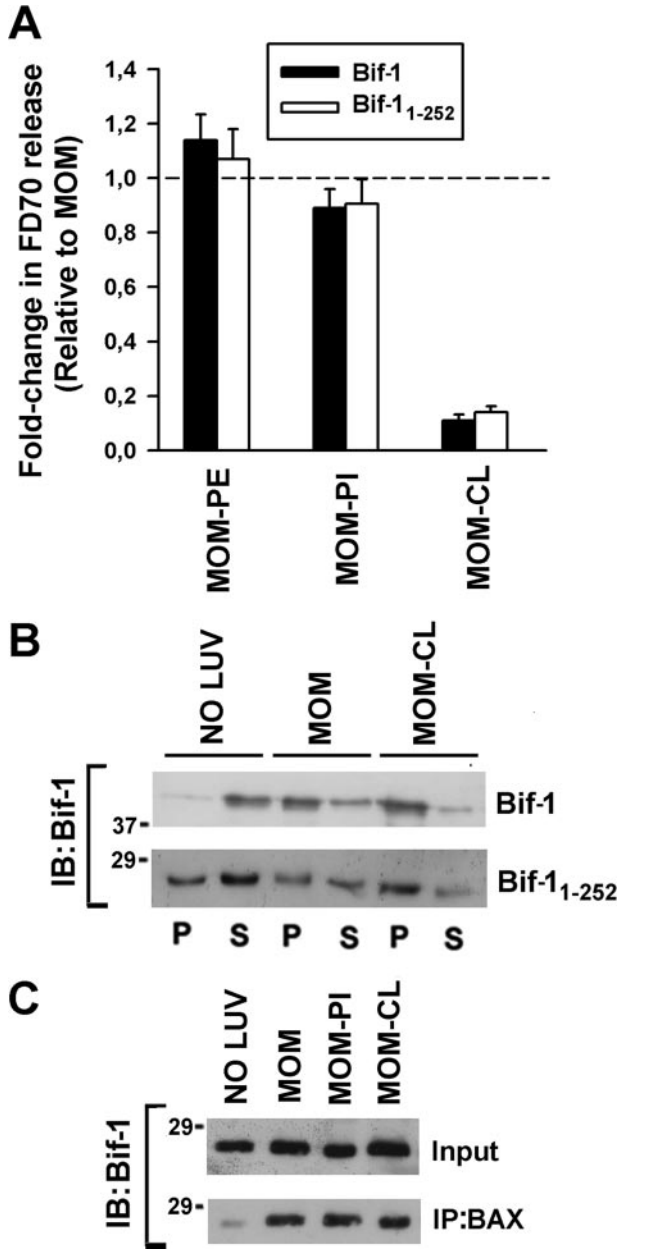

FIGURE 4. **Effect of membrane lipid composition on the potentiation of BAX-permeabilizing function elicited by Bif-1 N-BAR domain.** *A*, vesicular FD70 release induced by Bif-1 and Bif-1^{1-252} in MOM-like LUV in which indicated lipids were eliminated from the mixture, being substituted for equimolar amounts of PC. Liposome compositions were as follows: MOM-PE, 75 PC/10 PI/15 CL (mol/mol); MOM-PI, 50 PC/35 PE/15 CL (mol/mol); MOM-CL, 55 PC/35PE/10 PI (mol/mol). Data were normalized to the extents of vesicular FD70 release induced by Bif-1/Bif-1^{1-252} in MOM-like LUV (*dashed line*). Data represent the mean values and S.E. of 2–4 independent measurements. *B*, immunoblot analysis of the effect of CL on Bif-1/Bif-1^{1-252} association with MOM-like liposomes. Bif-1/Bif-1^{1-252} (400 nM) were incubated with BAX (100 nM) plus tBID (20 nM) alone or together with indicated liposomes, and liposomes were pelleted by centrifugation and analyzed for Bif-1/Bif-1^{1-252} contents in the liposome-containing (*P*) and liposome-free (*S*) fractions by immunoblotting. *C*, Bax (100 nM) and/or tBid (20 nM) were incubated with Bif-1^{1-252} (400 nM) in the presence or absence of indicated liposomes, and samples were immunoprecipitated (*IP*) using anti-BAX antibody conjugated to agarose beads and immunoblotted (*IB*) for Bif-1.

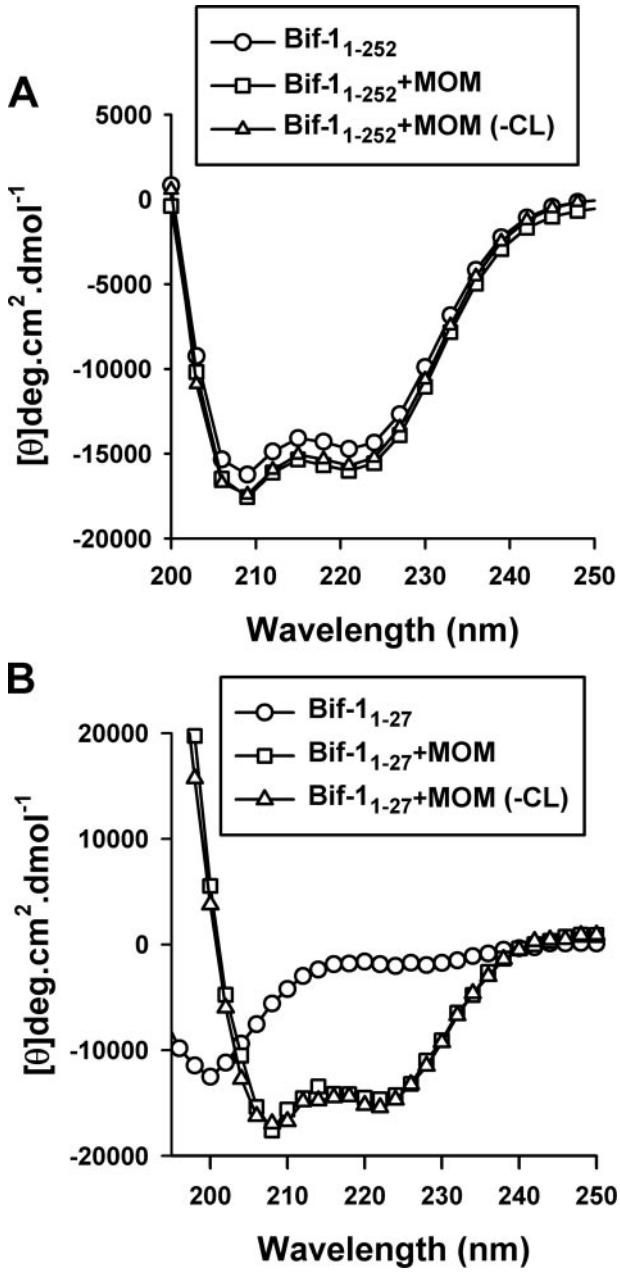

FIGURE 5. **Secondary structure of Bif N-BAR domain and H0 submodule in the presence of liposomes with different lipid composition.** Circular dichroism spectra of Bif-1^{1-252} (*A*) and Bif-1^{1-27} (*B*) taken in the presence or absence of small unilamellar vesicles composed of PC/PE/PI/CL (40/35/10/15) (*MOM*) or of PC/PE/PI (55/35/10/15) (*MOM (-CL)*).

insertion of amphipathic H0 and HI1 submodules of its N-BAR domain into the outermost leaflet of the bilayer (16, 17). Thus, we next evaluated the membrane-penetrating capacity of Bif-1

TABLE 1

Percent helicity of Bif-1 and different Bif-1 fragments in the absence and presence of liposomes with indicated lipid composition assessed by CD analysis

Results are the average of estimates from CONTINLL, SELCON3, and CDSSTR. The relative S.D. on the structural element prediction is typically 5–15%. The lowest relative S.D. are not associated with a particular structural element.

Protein/peptide	−LUV	+MOM SUV	+MOM SUV (−CL)
	%	%	%
Bif-1	38.1	37.3	39.8
Bif-1^{1-252}	53.5	64.3	63.6
Bif-$1^{253-361}$	5.3	11.1	12.9
Bif-1^{1-27}	4.2	54.5	56.6

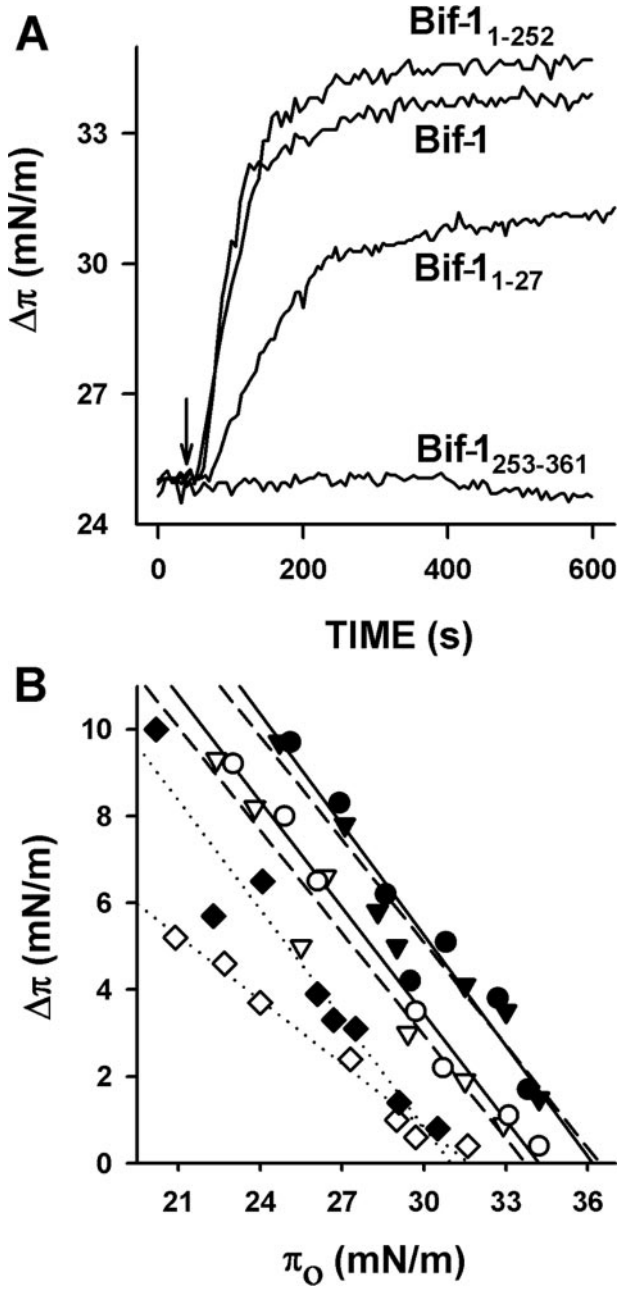

FIGURE 6. **Effect of Bif-1 and Bif-1 fragments on lipid monolayer surface pressure.** *A*, kinetics of Bif-1, Bif-1^{1-252}, and Bif-$1^{253-361}$ insertion into MOM-like lipid monolayers. *B*, surface pressure dependence of Bif-1 (*circles*), Bif-1^{1-252} (*triangles*), and Bif-1^{1-27} (*diamonds*) insertion into MOM-like monolayers containing (*filled symbols*) or devoid of CL (*empty symbols*). Curves for Bif-1 (*continuous*), Bif-1^{1-252} (*dashed*), and Bif-1^{1-27} (*dotted*) were determined by linear regression analysis; the intercept with the *x* axis defines the monolayer exclusion pressure.

and different fragments derived thereof. To this aim, a MOM-like lipid monolayer was spread at the air-water interface at an initial surface pressure of 25 millinewtons/m, and its surface pressure was monitored after injection into the subphase of Bif-1, Bif-1^{1-252}, Bif-$1^{253-361}$, or Bif-1^{1-27}. Both Bif-1 and Bif-1^{1-252} induced a rapid and prominent increase in the surface pressure of MOM-like monolayers, whereas Bif-1^{1-27} produced a slower and less pronounced increase in surface pressure, and Bif-$1^{253-361}$ had no activity in this assay (Fig. 6*A*). To obtain a quantitative measure of the penetration capacities of Bif-1 protein/fragments for entering MOM-like lipid monolayers, critical surface pressure values were determined. In these experiments, the increase in surface pressure ($\Delta\pi$)) upon protein/peptide addition was measured as a function of the initial surface pressure (Δ_0). As Δ_0 is increased, $\Delta\pi$ decreased upon Bif-1, Bif-1^{1-252}, and Bif-1^{1-27} addition (Fig. 6*B*). The data fit well to a straight line giving a critical surface pressure (π_c) of 36.1, 36.3, and 31. 7 millinewtons/m, for Bif-1, Bif-1^{1-252}, and Bif-1^{1-27}, respectively (Table 2). Elimination of CL from the lipid mixture significantly decreased π_c for Bif-1 and Bif-1^{1-252}, whereas Bif-1^{1-27} showed virtually identical exclusion pressures in monolayers with and without CL (Fig. 6*B* and Table 2). Nevertheless, because the surface pressure of liposomal membrane has been estimated to be ≥30 millinewtons/m (39), we infer from these results that Bif-1, its N-BAR domain, and the H0 submodule all can penetrate substantially into MOM-like LUV irrespective of the presence or absence of CL.

TABLE 2
Exclusion pressure of Bif-1 and different Bif-1 fragments in monolayers of indicated lipid composition

Protein/peptide	MOM	MOM (−CL)
	millinewtons/m	
Bif-1	36.1	34.2
Bif-1^{1-252}	36.3	33.7
Bif-1^{1-27}	31.7	31.2

Although electron microscopy can provide valuable information of the morphological changes induced by N-BAR domains in liposomes, it is often difficult to obtain quantitative data with this technique. In addition, electron microscopy requires the use of an adsorbed or fixed sample which may not accurately reflect the actual structures found in solution. Recent studies have shown that the N-BAR domain of endophilin A1 transforms spherical liposomes into narrow membrane tubules displaying high fusogenicity and that a FRET assay for intervesicular lipid mixing can be used as a quantitative readout of N-BAR-mediated membrane tubulation in solution (17). To investigate the ability of Bif-1 and fragments derived thereof to tubulate MOM-like LUV, liposomes containing PE lipids labeled in their headgroups with the NBD/rhodamine FRET pair were mixed with MOM LUV lacking fluorescent lipids under conditions such that FRET between fluorophores decreases on fusion with unlabeled liposomes. Both Bif-1 and Bif-1^{1-252}, but not Bif-$1^{253-361}$ or Bif-1^{1-27}, induced substantial intervesicular lipid mixing (Fig. 7*A*, *black bars*), consistent with the notion that Bif-1 shares with endophilin A1 the ability to bind to lipid bilayers and evaginate them into high curvature, fusogenic tubules via its N-BAR domain. In control experiments we found that the addition of Bif-1/Bif-1^{1-252} to a suspension of liposomes containing only labeled vesicles did not yield any significant effect in FRET (data not shown). To examine global morphological changes in liposomes by an independent readout in solution, we quantitatively monitored the size distribution of the vesicle suspension by DLS. Isolated MOM-like LUV showed a relatively narrow size distribution, with a mean ± S.D. diameter of 147.3 ± 31.2 nm (supplemental Fig. 3). In correlation with FRET results, treatment of vesicles with either Bif-1 or Bif-1^{1-252}, but not with Bif-$1^{253-361}$ or Bif-1^{1-27},

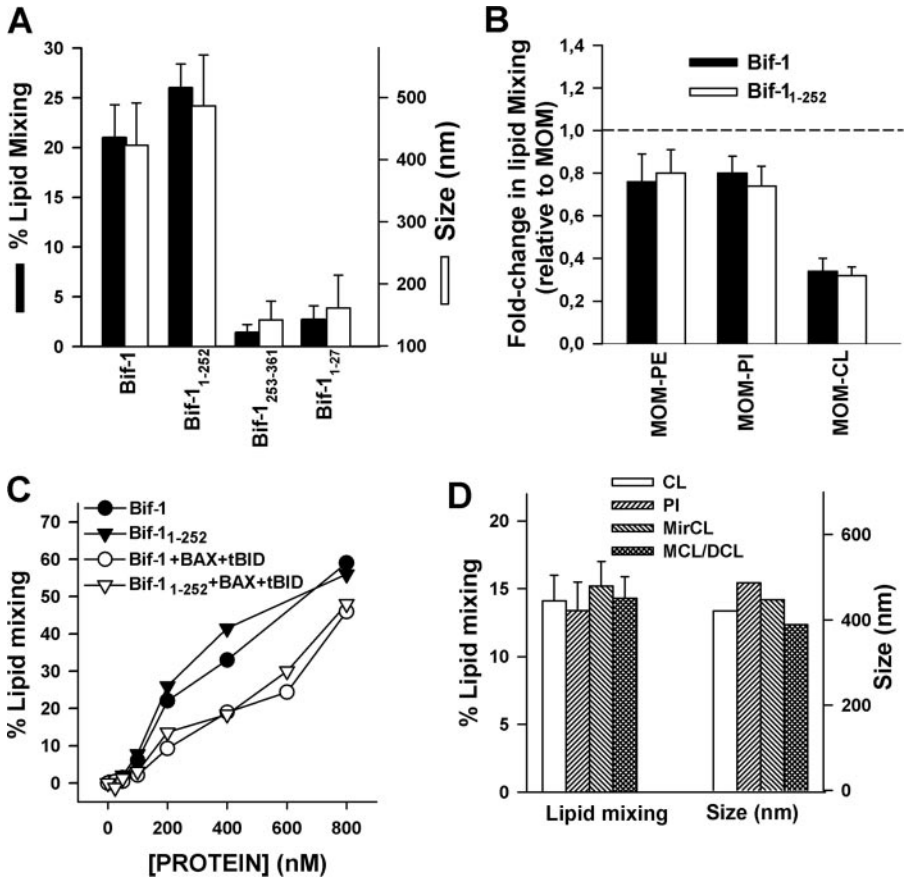

FIGURE 7. **Effect of Bif-1 and Bif-1 fragments on intervesicular lipid mixing and liposome size.** *A*, indicated proteins/peptides (200 nM) were incubated with MOM-like LUV followed by assessment of intervesicular lipid mixing (*filled bars*) and particle size distribution (*empty bars*) by FRET and DLS, respectively. Data represent mean values and S.E. of at least two independent measurements. *B*, effect of lipid composition on lipid mixing induced by Bif-1- and Bif-1 N-BAR domain in MOM-like LUV. Bif-1/Bif-1^{1-252} (200 nM) were incubated with liposomes in which indicated lipids were substituted by equimolar amounts of PC followed by determination of intervesicular lipid mixing by FRET. Data were normalized to the extents of lipid mixing induced by Bif-1/Bif-1^{1-252} in MOM-like LUV (*dashed line*). Data represent the mean values and S.E. of 2–4 independent measurements. *C*, dose dependence of intervesicular lipid mixing elicited by Bif-1 or Bif-1^{1-252} in MOM-like LUV in the absence or presence of BAX (50 nM) and tBID (10 nM). *D*, LUV composed of PC/PE/PI/CL (40/35/10/15) (*CL*), PC/PE/PI (40/35/40) (*PI*), PC/PE/PI/mirCL (40/35/10/15) (*MirCL*), or PC/PE/PI/MCL/DCL (40/35/10/7.5/7.5) (*MCL/DCL*) were treated with Bif-1^{1-252} (200 nM) together with BAX (50 nM) and tBID (10 nM) followed by determination of extents of intervesicular lipid mixing and liposome size distribution.

TABLE 3
Effect of lipid composition on membrane activities of Bif-1 N-BAR domain

Lipid (mol %)	Lipid mixing[a]	Liposome size[b]	Release[c]
	%	*nm*	
PC/PE/PI/CL (40/35/10/15)	26.3 ± 3.2	443 ± 63	2.47 ± 0.14
PC/PE/PI (25/35/40)	24.9 ± 4.5	483 ± 85	1.32 ± 0.12
PC/PE/PI/MirCL (40/35/10/15)	28.4 ± 3.8	522 ± 65	1.64 ± 0.09
PC/PE/PI/MCL/DCL (40/35/10/7.5/7.5)	23.1 ± 4.3	389 ± 58	1.71 ± 0.15

[a] Extents of intervesicular lipid mixing induced by Bif-1^{1-252} assessed by FRET.
[b] Values of mean liposome size ±S.E. (nm) obtained from DLS analysis of 2 independent vesicle populations.
[c] -Fold increase in the extent of vesicular FD70 release induced by Bif-1^{1-252} combined with 50 nM BAX plus 10 nM tBID normalized to that induced by 50 nM BAX plus 10 nM tBID alone. In all cases Bif-1^{1-252} and lipid concentrations were 200 nM and 50 mM, respectively.

increased liposome size distribution (Fig. 7*A*, *white bars*, and supplemental Fig. 3).

Notably, unlike the situation found in vesicular dextran release assays, elimination not only of CL but also of PE or PI from the MOM-like mixture reduced the amount of lipid mixing elicited by Bif-1^{1-252} (Compare Fig. 7*B* and Fig. 4*A*). These results raised the possibility that the large scale morphological rearrangements produced in MOM-like LUV by Bif-1 N-BAR might be uncoupled from its stimulatory effect on functional BAX activation. To further check this possibility and to advance in our understanding of the role played by CL in both processes, we analyzed the influence of the lipid environment in more detail. Specifically, we probed for the impact of CL replacement by (i) another anionic lipid (PI) while keeping the net charge of the vesicle equal to that existing in CL-containing MOM-like LUV, (ii) mirCL, which unlike CL, tends to segregate into a distinct phase when combined with unsaturated lipids (40) (supplemental Fig. 4), and (iii) derivatives of CL, which do not share with the parent lipid the potential to adopt a negatively curved nonlamellar disposition (MCL, DCL) (41, 42). Replacement of CL with PI, mirCL, or a MCL/DCL mixture did not change substantially the ability of Bif-1^{1-252} to induce intervesicular lipid mixing or to increase liposome size (Table 3). In contrast, replacement of CL with each one of these anionic lipids diminished the stimulation of BAX-permeabilizing function elicited by Bif-1^{1-252}. Thus, although the role of CL in Bif-1 N-BAR-mediated morphological rearrangements of MOM-like LUV could be ascribed to an electrostatic effect, other features of CL seem to underlie its requirement for Bif-1 N-BAR-mediated potentiation of BAX-permeabilizing function.

To further test for a relationship between the ability of Bif-1 N-BAR to reshape liposomes and its stimulatory effect on functional BAX activation, we examined the effect on liposome morphology elicited by Bif-1 and its N-BAR domain when combined with BAX and a suboptimal dosing of tBID. As shown in Fig. 7*C*, intervesicular lipid mixing decreased when MOM-like LUV were treated with Bif-1/Bif-1^{1-252} together with BAX and tBID, in contrast with the enhancement elicited by Bif-1/Bif-1^{1-252} in BAX-induced vesicular dextran release. Of note, the dependence of intervesicular lipid mixing on Bif-1/Bif-1^{1-252} dosing was different from that of vesicular dextran release (compare Fig. 7*C* and Fig. 3*B*). Furthermore, substitution of CL for PI, mirCL, or the MCL/DCL mixture had little effect on the intervesicular lipid mixing and on the increase of liposome size obtained when Bif-1 N-BAR was combined with BAX and tBID

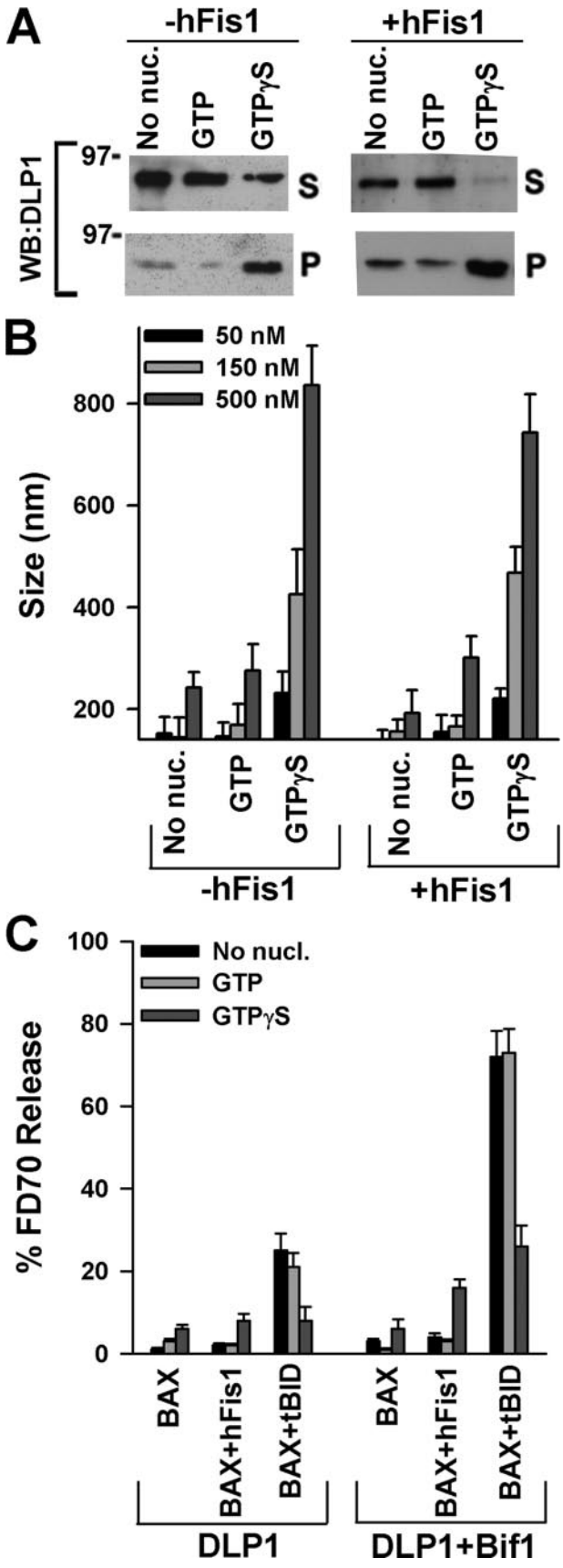

FIGURE 8. **Membrane activities of DLP1 and hFis1 in MOM-like LUV.** *A*, immunoblot analysis (*WB*) of DLP1 recruitment to MOM-like liposomes. DLP1 and freeze/thawed vesicles were incubated in KHE buffer with or without nucleotides and hFis1 followed by centrifugation of the mixture and immunodetection of DLP1 contents in the liposome-containing pellet (*P*) and liposome-free supernatant (*S*) fractions. Protein and nucleotide concentrations were 400 and 500 μM, respectively. *B*, MOM-like LUV were incubated with indicated amounts of DLP1 in KHE buffer with or without nucleotides and hFis1 (500 nM) followed by determination of liposome size by DLS. Data represent mean values and S.E. of duplicated measurements. *C*, assessment of DLP1 impact on BAX-permeabilizing function. DLP1 was incubated with indicated proteins and MOM-like LUV in KHE buffer with or without nucleotides followed by determination of vesicular FD70 release by spectrofluorimetry. DLP1, hFis1, Bif-1, BAX, and tBID concentrations were 400, 400, 200, 50, and 10 nM, respectively. Data represent mean values and S.E. of at least two independent measurements.

(Fig. 7*D*). Thus, we concluded that despite Bif-1 possesses the capacity to produce global changes in MOM-like LUV morphology via its N-BAR domain, this process can be separated from functional activation of proapoptotic BAX.

Large Scale Morphological Rearrangements of MOM-like LUV Induced by DLP1 Do Not Stimulate BAX-permeabilizing Function—Given that Bif-1 functions in normal MOM morphological dynamics together with DLP1/Drp1 (11) and that DLP1/Drp1 has been reported to contribute to BAX-driven MOMP during apoptosis (5–7), we next decided to examine the impact of DLP1/Drp1 on BAX-permeabilizing function in our liposomal reconstituted system. Of note, previous studies demonstrated that purified recombinant DLP1 alone can deform lipid vesicles into long membrane tubules in the presence of the non-hydrolyzable GTP analogue GTPγS (43). In the presence of GTPγS purified recombinant DLP1 associated with MOM-like liposomes and drastically increased liposome size as indicated by immunoblotting and DLS analysis (Fig. 8, *A* and *B*). Remarkably, however, GTPγS-treated DLP1 did not amplify but actually decreased the amount of vesicular FD70 elicited by BAX activated with a suboptimal dosing of tBID either in the absence or presence of Bif-1 (Fig. 8*C*). hFis1 is another component of the MOM fission machinery which has been suggested to recruit DLP1/Drp1 from the cytosol to the mitochondrial surface (34, 44) and to participate in functional BAX activation during apoptosis (4, 6). For the ease of purification, we obtained a recombinant form of hFis1 lacking a C-terminal hydrophobic domain which maintains the capacity to bind DLP1 (34). Treatment of MOM-like liposomes with recombinant hFis1 only produced a slight increase in the amount of DLP1 recruited with lipid vesicles (Fig. 8*A*), and the hFis1 plus DLP1 mixture had little effect on BAX-induced vesicular dextran release in the absence or presence of Bif-1 (Fig. 8*C*).

In summary, no evidence was obtained supporting that DLP1 alone or in cooperation with hFis1/Bif-1 promotes BAX-induced vesicular dextran release in MOM-like LUV. Additionally, these results add further support to the notion that large scale morphological rearrangements of MOM-like LUV elicited by components of the mitochondrial morphogenesis machinery are not linked to functional BAX activation.

DISCUSSION

In the intrinsic apoptotic pathway, the BCL-2 family of proteins regulates the release of mitochondrial intermembrane space proteins into the cytosol with the assistance of an increasing number of regulatory factors, among which components of the mitochondrial morphogenesis machinery stand out (2–4).

Given the complexity of studies with living cells at compositional, structural, and dynamic levels, a comprehensive mechanistic understanding of the apoptotic role played by specific proteins requires the capacity to reconstitute their pro-death function into simplified and biochemically accessible systems allowing precise controls over experimental conditions. In this study we used a reconstituted liposomal system that faithfully recapitulates basic physiological aspects of the BCL-2-regulated MOMP pathway to learn more about the mode of Bif-1 action in apoptosis.

Using this reductionist model system, we provide for the first time direct evidence that Bif-1 possesses the intrinsic capacity to stimulate the permeabilizing function of BAX by conformationally activating BAX at the membrane level. We also show that Bif-1 directly interacts with BAX in the presence of MOM-like liposomes but not in solution and that both the physical and the functional interaction between Bif-1 and BAX require "priming" of soluble BAX by other apoptotic stimuli (tBID/heat exposure) that trigger BAX membrane recruitment. These results mesh well with previous studies in cells revealing that the interaction between Bif-1 and BAX occurs only upon apoptotic stimulation, being detected primarily at the mitochondria rather than in the cytoplasm (12, 13, 36). Because the BAX-driven membrane permeabilization pathway in MOM-like LUV triggered by tBID and/or heat exposure appears to be initiated by unleashing of a carboxyl-terminal membrane-anchoring helix of BAX (α9) (31), the incapacity of Bif-1 for binding BAX in solution may be due to occlusion of critical Bif-1-interacting residues by BAX α9. Yeast-two hybrid studies mapping the binding region between Bif-1 and BAX lacking α9 are consistent with this possibility (37), although the data available do not allow reaching a definitive conclusion. Alternatively, or in addition, membrane targeting may facilitate BAX association with the Bif-1 BAX binding motif (which we termed BBM) due to increased local concentration of the two proteins at the liposomal surface.

In this study we also report that Bif-1 stimulates BAX-permeabilizing function via its N-BAR domain, which in addition to holding a BBM confers capacity to the protein for producing large scale morphological rearrangements in liposomes containing anionic lipids, as previously described for other N-BAR-containing proteins (14–18). Such common activity of N-BAR-containing proteins has been linked to their cooperative action with different binding partners in membrane remodeling events occurring during normal cell growth (14–19, 27, 29). In support of this notion, endophilin A1 is known to cooperate with dynamin, creating tubular plasma membrane extensions and inducing vesicle budding during endocytosis (16–19), whereas Bif-1 works together with DLP1/Drp1 to maintain normal tubulovesicular morphological MOM dynamics in healthy cells (11).

Importantly, we obtained three lines of evidence in our reconstituted system uncoupling large scale rearrangements of liposome morphology produced by components of the mitochondrial morphogenesis machinery from potentiation of functional BAX activation. First, we found that intervesicular lipid mixing and potentiation of BAX-permeabilizing function do not exhibit the same dependence on Bif-1/Bif-1 N-BAR dosing, with the former process requiring higher protein amounts than the latter one. Second, we showed that the membrane lipid composition has a distinct impact on the liposome-reshaping and BAX-activating functions of Bif-1 N-BAR. The finding that several different anionic lipids providing the same net negative charge to the membrane similarly affect the ability of Bif-1 N-BAR to induce intervesicular lipid mixing and to increase liposome size is consistent with the view that electrostatic interactions between positively charged residues localized in the concave surface of this module and negatively charged phospholipid headgroups is a major factor driving liposome morphological rearrangements, as previously proposed for N-BAR domains of other proteins (15, 16, 20, 21, 23). In contrast, an electrostatic effect alone does not explain the requirement of CL for the potentiation of BAX-permeabilizing function elicited by Bif-1 N-BAR, in accord with previous studies indicating that other properties of CL account for its specific role in functional BAX activation (30, 31, 45, 46). Third, although we confirmed that DLP1 itself has the capacity to produce global changes in liposome morphology (43), we established that this protein does not potentiate BAX-permeabilizing function in the absence or presence of hFis1 and/or Bif-1. A cautionary note here is that we cannot rule out that other factors might affect the inability of DLP1 to enhance BAX-permeabilizing function in our model experimental system. These include a possible involvement of additional mitochondrial components (proteins and/or lipids) and the lack of post-translational modifications in DLP1.

There exist multiple possibilities to explain how the Bif-1 N-BAR domain may stimulate functional BAX activation in MOM-like LUV independently from its ability to produce large scale morphological changes in these vesicles. Although our results clearly showed that protein-protein interactions are implicated in the functional interplay between Bif-1and BAX, CL also seems to play a key role in this process. One possibility is that the presence of CL in the membrane may allow Bif-1 N-BAR to adopt the orientation and/or stoichiometry required for establishing productive interactions with BAX. An alternative view is that the interaction of Bif-1 N-BAR with CL produces localized changes in membrane structure distinct from the large scale membrane morphological rearrangements detected by FRET and DLS assays, which in turn facilitate conformational activation of BAX. In this regard we note that (i) unlike PI, MCL, or DCL, CL has the potential to shift from a lamellar to a negatively curved nonlamellar configuration upon charge neutralization via interaction with polybasic peptides/proteins (41, 42, 47) and that (ii) the presence of negatively curved nonlamellar lipids in the bilayer can cause conformational changes in membrane proteins (48). Yet, another plausible explanation, not necessarily incompatible with the previous proposals, is that by interacting simultaneously with BAX via the BBM and with CL via the basic concave surface, Bif-1 N-BAR concentrates CL in the vicinity of BAX thereby indirectly stimulating functional BAX activation. From this perspective, the diminished potentiating effect of Bif-1 N-BAR in MOM-like LUV containing mirCL instead of CL could be explained by the capacity of the former but not the later lipid to phase-separate in mixtures with unsaturated phospholipids

(supplemental Fig. 4), as this would eliminate the requirement of Bif-1 for recruiting BAX to mirCL-enriched domains.

We have focused our experiments on model membrane systems emulating the lipid composition of CL-enriched mitochondrial membrane contact sites, which have been implicated in a variety of healthy and apoptotic functions of the organelle (49, 50). However, our studies do not necessarily imply that the functional interaction between BAX and Bif-1 occurs at these mitochondrial structures. Considering the evidence indicating that CL is translocated from the mitochondrial inner membrane to the MOM at early stages of the apoptotic pathway (51–53), it is not unreasonable to speculate that during apoptosis Bif-1 and BAX might interact at CL-enriched microdomains of the MOM distinct from "classical" mitochondrial membrane contact sites. Clearly, further work is required to determine the precise mitochondrial localization of Bif-1, BAX, and CL under healthy and apoptotic conditions.

In conclusion, we propose a model whereby during apoptosis Bif-1 works in concert with CL at the MOM level to enhance BAX-driven MOMP, thereby allowing robust egress of intermembrane space proteins into the cytosol. We further suggest that this proapoptotic function of MOM-localized Bif-1 is independent from the role played by this protein together with DLP1 when producing global MOM shape changes in healthy cells. Additional components of the mitochondrial shaping machinery have been proposed to possess proapoptotic functions that are unrelated to their recognized roles in normal mitochondrial dynamics, which converge at the level of restructuring the mitochondrial inner membrane to mobilize cytochrome *c* sequestered within cristae folds (8–10, 54, 55). It should be stressed, however, that MOMP has other lethal consequences in addition to cytochrome *c* release and that MOMP and not cytochrome *c* release alone appears to be the irreversible commitment point to cell death for the majority of apoptotic stimuli (1, 56, 57).

Acknowledgments—We thank Dr. Y. Yoon (University of Rochester School of Medicine and Dentistry, Rochester, NY) for the generous gifts of plasmids for expression of DLP1 and hFis1 proteins as well as J. Sot (Unidad de Biofísica, CSIC-Universidad del Pais Vasco/Euskal Herriko Unibertsitatea) for technical assistance with fluorescence microscopy studies.

REFERENCES

1. Green, D. R., and Kroemer, G. (2004) *Science* **305,** 626–629
2. Youle, R. J., and Strasser, A. (2008) *Nat. Rev. Mol. Cell Biol.* **9,** 47–59
3. Chipuk, J. E., and Green, D. R. (2008) *Trends Cell Biol.* **18,** 157–164
4. Suen, D.-F., Norris, K. L., and Youle, R. J. (2008) *Genes Dev.* **22,** 1577–1590
5. Frank, S., Gaume, B., Bergmann-Leitner, E. S., Leitner, W. W., Robert, E. G., Catez, F., Smith, C. L., and Youle, R. J. (2001) *Dev. Cell* **1,** 515–525
6. Lee, Y. J., Jeong, S. Y., Karbowski, M., Smith, C. L., and Youle, R. J. (2004) *Mol. Biol. Cell* **15,** 5001–5011
7. Cassidy-Stone, A., Chipuk, J. E., Ingerman, E., Song, C., Yoo, C., Kuwana, T., Kurth, M. J., Shaw, J. T., Hinshaw, J. E., Green, D. R., and Nunnari, J. (2008) *Dev. Cell* **14,** 193–204
8. James, D. I., and Martinou, J. C. (2008) *Dev. Cell* **15,** 341–343
9. Germain, M., Methai, J. P., McBride, H. M., and Shore, G. (2005) *EMBO J.* **24,** 1546–1556
10. Alirol, E., James, D., Huber, D., Marchetto, A., Vergani, L., Martinou, J. C., and Scorrano, L. (2006) *Mol. Biol. Cell* **17,** 4593–4605
11. Karbowski, M., Jeong, S.-Y., and Youle, R. J. (2004) *J. Cell Biol.* **27,** 1027–1039
12. Takahashi, Y., Karbowski, M., Yamaguchi, H., Kazi, A., Wu, J., Sebti, S. M., Youle, R. J., and Wang, H. G. (2005) *Mol. Cell. Biol.* **25,** 9369–9382
13. Cuddeback, S. M., Yamaguchi, H., Komatsu, K., Miyashita, T., Yamada, M., Wu, C., Singh, S., and Wang, H. G. (2001) *J. Biol. Chem.* **276,** 20559–20565
14. Farsad, K., Ringstad, N., Takei, K., Floyd, S. R., Rose, K., and De Camilli, P. (2001) *J. Cell Biol.* **155,** 193–200
15. Peter, B. J., Kent, H. M., Mills, I. G., Vallis, Y., Buttler, P. J. G., Evans, P. R., and McMahon, H. T. (2004) *Science* **303,** 495–499
16. Masuda, M., Takeda, S., Sone, M., Ohki, T., Mori, H., Kamioka, Y., and Mochizuki, N. (2006) *EMBO J.* **25,** 2889–2897
17. Gallop, J. L., Jao, C. C., Kent, H. M., Butler, P. J., Evans, P. R., Langen, R., and McMahon, H. T. (2006) *EMBO J.* **25,** 2898–2910
18. Weissenhorn, W. (2005) *J. Mol. Biol.* **351,** 653–656
19. Antonny, B. (2006) *Curr. Opin. Cell Biol.* **18,** 386–394
20. Blood, P. D., and Voth, G. A. (2006) *Proc. Natl. Acad. Sci. U. S. A.* **103,** 15068–15072
21. Ayton, G. S., Blood, P. D., and Voth, G. A. (2007) *Biophys. J.* **92,** 3595–3602
22. Campelo, F., McMahon, H. T., and Kozlov, M. M. (2008) *Biophys. J.* **95,** 2325–2339
23. Blood, P. D., Swenson, R. D., and Voth, G. A. (2008) *Biophys. J.* **95,** 1866–1876
24. Löw, C., Weininger, U., Lee, H., Schweimer, K., Neundorf, I., Beck-Sickinger, A. G., Pastor, R. W., and Balbach, J. (2008) *Biophys. J.* **95,** 4315–4323
25. Frolov, V. A., and Zimmerberg, J. (2008) *Cell* **132,** 727–729
26. Modregger, J., Schmidt, A., Rittere, B., Huttner, W. B., and Plomman, M. (2003) *J. Biol. Chem.* **278,** 4160–4167
27. Yang, J. S., Zhang, L., Lee, S. Y., Gad, H., Luini, A., and Hsu, V. W. (2006) *Nat. Cell Biol.* **8,** 1376–1382
28. Takahashi, Y., Coppola, D., Matsushita, N., Cualing, H. D., Sun, M., Sato, Y., Liang, C., Jung, J. U., Cheng, J. Q., Mul, J. J., Pledger, W. J., and Wang, H. G. (2007) *Nat. Cell Biol.* **9,** 1142–1151
29. Wan, J., Cheung, A. Y., Fu, W. Y., Wu, C., Zhang, M., Mobley, W. C., Cheung, Z. H., and Ip, N. Y. (2008) *J. Neurosci.* **28,** 9002–9012
30. Kuwana, T., Mackey, M. R., Perkins, G., Ellisman, M. H., Latterich, M., Schneiter, R., Green, D. R., and Newmeyer, D. D. (2002) *Cell* **111,** 331–342
31. Terrones, O., Etxebarria, A., Landajuela, A., Landeta, O., Antonsson, B., and Basañez, G. (2008) *J. Biol. Chem.* **283,** 7790–7803
32. Basañez, G., and Hardwick, J. M. (2008) *PloS Biol.* **6,** e154
33. Billen, L. P., Kokoski, C. L., Lovell, J. F., Leber, B., and Andrews, D. W. (2008) *PLoS Biol.* **6,** 1268–1280
34. Yoon, Y., Krueger, E. W., Oswald, B. J., and McNiven, M. A. (2003) *Mol. Cell. Biol.* **23,** 5409–5420
35. Struck, D. K., Hoekstra, D., and Pagano, R. E. (1981) *Biochemistry* **20,** 4093–4099
36. Yamaguchi, H., Woods, N. T., Dorsey, J. F., Takahashi, Y., Gjertsen, N. R., Yeatman, T., Wu, J., and Wang, H. G. (2008) *J. Biol. Chem.* **283,** 19112–19118
37. Pierrat, B., Simonen, M., Cueto, M., Meston, J., Ferrigno, P., and Heim, J. (2001) *Genomics* **71,** 222–234
38. Habermann, B. (2004) *EMBO Rep.* **5,** 250–255
39. Marsh, D. (1996) *Biochim. Biophys. Acta* **1286,** 182–223
40. Lewis, R. N., Zweytick, D., Pabst, G., Lohner, K., and McElhaney, R. N. (2007) *Biophys. J.* **92,** 3166–3177
41. Powell, G. L., and Marsh, D. (1985) *Biochemistry* **24,** 2902–2908
42. Dahlberg, M. (2007) *J. Phys. Chem.* **111,** 7194–7200
43. Yoon, Y., Pitts, K. R., and McNiven, M. A. (2001) *Mol. Biol. Cell* **12,** 2894–2905
44. Wells, R. C., Picton, L. K., Williams, S. C. P., Tan, F. J., and Hill, R. B. (2007) *J. Biol. Chem.* **282,** 33769–33775
45. Terrones, O., Antonsson, B., Yamaguchi, H., Wang, H. G., Liu, J., Lee, R. M., Herrmann, A., and Basañez, G. (2004) *J. Biol. Chem.* **279,** 30081–30091
46. Lucken-Ardjomande, S., Montessuit, S., and Martinou, J. C. (2008) *Cell*

Death Differ. **15,** 929–937
47. Basañez, G. (2002) *Cell. Mol. Life Sci.* **59,** 1478–1490
48. van den Brink-van der Laan, E., Killian, J. A., and de Kruijff, B. (2006) *Biochim. Biophys. Acta* **1666,** 275–288
49. Reichert, A. S., and Neupert, W. (2002) *Biochim. Biophys. Acta* **1542,** 41–49
50. Scorrano, L. (2008) *J. Cell Biol.* **183,** 579–581
51. Kagan, V. E., Tyurin, V. A., Jiang, J., Tyurina, Y. Y., Ritou, V. D., Amoscato, A. A., Osipov, A. N., Belikova, N. A., Kapralov, A. A., Kini, V., Vlasova, I. I., Zhao, Q., Zou, M., Di, P., and Borisenko, G. G. (2005) *Nat. Chem. Biol.* **1,** 223–232
52. Liu, J., Dai, Q., Chen, J., Durrant, D., Freeman, A., Liu, T., Grossman, D., and Lee, R. M. (2003) *Mol. Cancer Res.* **1,** 892–902
53. Liu, J., Epand, R. F., Durrant, D., Grossman, D., Chi, N. W., Epand, R. M., and Lee, R. M. (2008) *Biochemistry* **47,** 4518–4529
54. Frezza, C., Cipolat, S., Martins de Brito, O., Micaroni, M., Beznoussenko, G. V., Rudka, T., Bartoli, D., Polishuck, R. S., Danial, N. N., De Strooper, B., and Scorrano, L. (2006) *Cell* **126,** 177–189
55. Yamaguchi, R., Lartigue, L., Perkins, G., Scott, R. T., Dixit, A., Kushnareva, Y., Kuwana, T., Ellisman, M. H., and Newmeyer, D. D. (2008) *Mol. Cell* **31,** 557–569
56. Sheridan, C., and Martin, S. J. (2008) *Trends Cell Biol.* **18,** 353–357
57. Solary, E., Giordanetto, F., and Kroemer, G. (2008) *Nat. Genet.* **40,** 379–380